ROLE OF SURFACE CHEMISTRY IN SUB-EINSTEIN RHEOLOGY OF NANO-COMPOSITES

BY

MOULIK A. RANKA

THESIS

Submitted in partial fulfillment of the requirements
for the degree of Master of Science in Chemical Engineering
in the Graduate College of the
University of Illinois at Urbana-Champaign, 2012

Urbana, Illinois

Adviser:

Professor Charles F. Zukoski

ABSTRACT

Sub-Einstein and negative intrinsic viscosities resulting from the addition of nano-fillers to polymer melts approximately 2-10 nm diameter have been reported. Here we explore the intrinsic viscosity of polyhedral oligomeric silisequioxane (POSS) particles of approximately 1.6-2.5 nm diameters as a function of polymer molecular weight. These nanoparticles consist of cubes of 8-corner silicon atoms edge bridged with oxygen atoms. A variety of functional groups are attached to the corner silicon atoms. Three different POSS particles are explored: POSS with 8 tethered alkyl chains (butyl and octyl) and POSS with 8 tethered polyethylene glycol, PEG, chains of degree of polymerization, n ~ 13 segments. The tethered particles are dissolved in a homopolymer matrix (polydimethyl siloxane, PDMS, for octyl-POSS and butyl-POSS and PEG for PEG-POSS). The POSS intrinsic viscosity drops with increasing polymer matrix molecular weight from approximately 2.5 (as predicted by Einstein for no slip boundary conditions) to negative values. We discuss these results in light of previous studies of the intrinsic viscosity of nanoparticles in polymer melts with special attention to particle-polymer segment surface interactions that result in particle-polymer miscibility and ideas based on the ability of nanoparticles to alter polymer relaxation rates. We develop a hypothesis that negative intrinsic viscosities are associated with weak particle-polymer segment surface interactions while at the same time developing mechanisms that ensure particles remain soluble in the polymer melt.

ACKNOWLEDGEMENTS

This thesis would not have been possible without the guidance, enthusiasm and patience shown by my advisor, Professor Charles Zukoski. I would like to thank him for the many hours spent with him discussing the work, which has made its way into this thesis as well as for the many revisions that he helped me make. I would also like to thank him for the family atmosphere he created within the group, which made associating with him at work and outside truly enjoyable and I wish him all the best in his future endeavors as Provost. I would also like to thank So Youn Kim for all her help in learning the use of tools for analyzing scattering data and helping me understand her previous work, which my study builds upon. I would like to thank Nikola Dudukovic for volunteering the excellent assistance he provided me in collecting scattering data at Argonne National Lab without which it would not have been possible to prepare and run as many samples as I did. I would also like to thank Steve Weigand and Argonne National Lab for providing support for and use of beamline 5ID. Lastly I would like to thank the Department of Chemical and Biomolecular Engineering at the University of Illinois, Urbana-Champaign for giving me the chance to pursue this work and for providing me world-class education and opportunities and for which I am truly grateful.

TABLE OF CONTENTS

CHAPTER 1: INTRODUCTION AND BACKGROUND

INTRODUCTION

Composites are multiphase materials of at least two or more chemically or mechanically distinct phases, where one phase is dispersed in another at a macroscopic or microscopic scale. The idea behind the composite is to synergistically combine two materials such that each phase compensates for the drawbacks related with the other. For example, inorganics have extremely high tensile strength but are brittle whereas polymers have a much lower tensile strength but are much tougher and less prone to fracture. By combining the two, provided there is good dispersion of the inorganic phase, one is able to obtain materials with higher tensile strength than that of the polymer and less brittle than the inorganic phase.

Composites are all around us. They can be seen most commonly in the form of inorganic filler reinforced polymers all around us such as tires, plastic pipes, fire resistant jacketed cables etc. Other forms of composites include metal-ceramic composites for high temperature applications, glass and carbon fiber reinforced resins used in high mechanical performance applications such as airplane and car parts and windmill blades. Composites also occur in nature such as wood for example, which is a composite of cellulose fibers contained within a matrix of lignin[1], or bone which is a composite of hydroxyapatite in a matrix of collagen[2]. In both cases, the dual phase nature is key to their function of withstanding the external stresses and strains from the environment.

The properties of composite materials vary based on factors such as chemical nature of the filler, its dispersion in the matrix as well as the filler aspect ratio. Properties that are affected due to filler incorporation include but are not limited to electrical and thermal conductivity, optical properties, dielectric properties, resistance to heat, mechanical properties such as tensile strength, elongation, tear resistance, hardness, stiffness, and abrasion resistance. In recent years composites made from nano-fillers have become more relevant as the small size of the filler phase imparts significant changes in properties such as discussed above with as little as 5 percent of filler incorporated by volume[3]. Nano fillers are defined by having at least one of the three dimensions being less than 100nm in length[3]. Examples include clays, carbon black, metal and

metal oxide particles that meet these criteria. The reason for this is the extremely high surface area-to-volume ratio of these fillers that allows for very close distance of separation between the particles and thus have a very low percolation threshold giving rise to interesting phenomenon such as electrical conductivity at very low volume fractions, or drops in viscosity of the polymer melt due to possibly altering the physical state of the polymer matrix[4].

The effect of lowered viscosity as more nano-fillers are introduced in a polymer matrix is of particular interest and the study of this phenomenon is the main aim of the thesis. Work by Mackay[4] and Cosgrove[8] suggests that when surface to surface separation of the particles dispersed in a polymer melt is equal to or less than the radius of gyration Rg of the bulk polymer, and the polymer is above its entanglement molecular weight, the polymer chains that are confined between the particles are forced to adopt configurations not seen in the absence of particles. One hypothesis is that this results in chains that are disentangled and aligned thus decreasing the polymer relaxation time and reducing the polymer viscosity. This disentanglement of the polymer thus causes composite viscosity to be lower than that of the melt resulting in the particles having a negative intrinsic viscosity [η]. As [η] represents the energy dissipated per particle and is associated with increased shear rates near a particle surface in the presence of shear, a negative value is difficult to reconcile with the standard continuum perspective that results in the Einstein intrinsic viscosity of 2.5 for particles suspended in a Newtonian continuous phase experiencing a no slip boundary condition and an intrinsic viscosity of 1 if the particle experiences a slip boundary condition with the solvent[5].

We aim to study that the phenomenon of negative intrinsic viscosities induced by nano-particles dispersed in polymer melts which is against the predictions of classical colloidal science. Although particle-polymer systems displaying negative intrinsic viscosities have been seen before, the exact mechanism by which this occurs is still not fully understood. We discuss these results in light of previous studies of the intrinsic viscosity of nanoparticles in polymer melts with special attention to particle-polymer segment surface interactions that result in particle-polymer miscibility and ideas based on the ability of nanoparticles to alter polymer relaxation rates. We develop a hypothesis that negative intrinsic viscosities are associated with weak particle-polymer segment surface interactions while at the same time developing mechanisms that ensure particles remain soluble in the polymer melt. We further aim to corroborate our experimental observations with models that have been proposed[9].

COLLOIDS IN LOW MOLECULAR WEIGHT SOLVENTS

Colloids are defined as a certain material phase that is evenly dispersed throughout another distinct material phase on a size scale of 1 to 1000 nanometers of the dispersed phase. The material that is evenly distributed is known as the dispersed phase and the material in which it is dispersed is known as the continuous phase. The dispersed and the continuous phases each could be any of three phases that are: solid, liquid and gas.

Examples of liquid in liquid colloids are oil-in-water or water-in-oil emulsions such as mayonnaise. An example of a liquid in gas colloidal mixture is fog or aerosols. Solid in liquid colloids are by far the most common and include examples such as muddy water, toothpaste, finely processed food pastes, paints, and polymer composite melts. This study shall be focused on solid-in-liquid colloidal suspensions where the continuous phase can be a low molecular weight solvent or a polymer with a degree of polymerization from below to above its entanglement value.

The rheology of colloidal suspensions is of particular importance to the industry due to its high tunability. The rheology of colloids is highly dependent on factors such as volume fraction, particle interactions, state of aggregation and particle-solvent/polymer interactions. By exerting control over these factors by careful formulation of the suspension, one is able to create systems that exhibit rheology suitable for a particular application. For example, the understanding and ability to tune the rheology of systems has allowed for industry to produce pastes that flow easily upon exertion of stress, but that do not sag in the absence of an externally applied shear stress. Examples include toothpaste, cosmetic creams, ketchup etc. Rheology is very important when designing a good paint since it too must be able to flow and spread easily but at the same time not drip when applied to walls. Paints must also undergo easy leveling so as to produce a smooth finish. Therefore, an understanding of colloids and the above mentioned factors are very important control over the flow properties of the system is required.

Investigation into the properties of colloidal systems began in the early 19th century with the study of Brownian motion aptly named after Robert Brown, a botanist, who observed suspended particles moving around in a random manner under the microscope[10]. This was due to the random collisions of the continuous liquid medium with the colloid particles. Thomas Graham did further investigation of colloids in the 1860s. He deducted that some of the major

characteristics of colloids included low diffusivity, the absence of crystallinity and lack of ordinary chemical relations[11].

Colloidal interactions, which ultimately decide the systems rheological properties, are based on the following forces[12]:

1) Volume Exclusion Repulsion – This is the repulsion resulting from short-range repulsions developed between electron clouds of atoms on different particles. When the range of this repulsion is much smaller than the particle size, the particles are said to be hard experiencing no direct interactions until there is contact where the particles feel an infinite repulsive potential.
2) Electrostatic Interaction – The colloid particles may carry charges, either similar or opposite that could give rise to repulsions or attractions. The magnitude of the force is also dependent on the charge density of the colloidal phase and the range is controlled by the continuous phase ionic strength.
3) Van der waals Forces – These forces are short-range attractive forces that arise due to temporary induced dipoles between atoms in the different particles. These can be screened if the particles and the continuous medium have similar refractive indices.
4) Entropic Forces – The colloidal system tends to maximize its entropy and thus any local order may create driving forces towards higher entropy. These interactions are particularly important in the case of a mixture of particles, solvent and polymer where confining polymer between two particle surfaces lowers the polymer entropy. However if the particles move close together and exclude the polymer, the volume available to the polymer is maximized thus maximizing its entropy.
5) Steric Repulsions – These repulsions result for a reduction in the entropy of polymer chains adsorbed or grafted to the particle surface. When two particles approach, the configurations of the adsorbed or grafted polymer chains are restricted again decreasing their entropy and producing a repulsive inter-particle force.

If the colloidal system of hard spheres is so dilute that each particle can be considered suspended in infinite continuous medium, and if the system is istropic in structure, according to Einstein[5] in 1906, the effective viscosity of the system,

$$\eta_{eff} = \eta_s (1 + 2.5\Phi)$$

where η_s is the solvent viscosity and Φ is the volume fraction of particles in the suspension. The equation may also be written as:

$$(\eta_{eff} - \eta_s) / \eta_s = [\eta]\Phi$$

where for the above limiting case as described, $[\eta]$ which is also known as the intrinsic viscosity which equals 2.5 for hard spheres experiencing a no-slip boundary condition. For colloids at higher volume fractions, characterizing the rheology of the dispersion requires the knowledge of the hydrodynamic and direct interparticle forces the resulting microstructure of the system and a method to calculate the macroscopic stress from the above information. A complete theory that includes hydrodynamic interactions for hard spheres and brownian motion was given by Batchelor[6] showing that:

$$\eta_{rel} = \eta_{eff} / \eta_s = 1 + 2.5\,\Phi + 6.2\,\Phi^2$$

where η_{rel} is the *relative viscosity*. The equation above may also be written as:

$$(\eta_{rel} - 1) / \Phi = 2.5 + k_H\,\Phi$$

where the left hand side of the equation is also known as *reduced viscosity* and k_H is known as the Huggin's coefficient[13]. In case of Batchelor's model that only takes into account the hydrodynamic and Brownian interactions, k_H = 6.2, where of that, 2.5 is from near-field hydrodynamic interactions, 2.7 from far-field hydrodynamic interactions and 1 from Brownian motion. It has been seen that in the case of sticky sphere interactions (where the contact potential between hard spheres is taken as $-\infty$ and zero elsewhere) and excluded shell interactions, the Huggin's coefficient tends to increase. Wagner et al[14] later studied the effect of square well and square pillar potential interactions on the Huggin's coefficient and showed that the increase of attraction as well as repulsion forces tend to cause an increase in the Huggin's coefficient but the increase due to attractions is of a much greater magnitude as compared to that from repulsions. It is important to note that the intrinsic viscosity is a single particle effect. It represents the increase in energy dissipation due to addition of particles in the infinitely dilute limit. The Huggins coefficient is a measure of pair interactions. In looking at the effect of nanoparticles on nanocomposite melt viscosity; the linear term $[\eta]$ is associated with how single

particles impact the composite stress relaxation processes while the Huggins coefficient indicates how pairs of particles interact and alter energy dissipation. Thus all the physics that are studied are done so from a single particle perspective. The viscosity measurements are thus done only in the low volume fraction limit, where particles are far away from each other so as to not induce multi-particle effects.

Nanocomposites as discussed in this study are composed of particles suspended in a polymer matrix with a large number of degrees of freedom. However due to the systems being studied being Newtoninan, and thus understanding a low molecular weight solvent system containing particles with large degree of freedom is a good place to start in order to characterize the nano-composite system.

COLLOIDS IN POLYMER MELTS

Just as the area of colloidal suspensions in low molecular weight solvents has garnered much interest and investigation since the early 20^{th} century, due to its varied practical applications in the industry such as delivery systems, rheology modifiers etc., the focus has over the years shifted to colloidal systems in polymer melts. As time has progressed, society has demanded materials with more unique functionalities, durability, and other properties that are only accomplished through the use of composite materials. Composite materials as stated earlier are materials where, in the most common case, fillers of inorganic origin which are extremely hard but brittle and suspended in a matrix of polymers that provide toughness to the composite material. Theories of colloidal science are thus applicable to such systems albeit in a manner modified to take into account the physics of such suspensions. This could be, for example, the relaxation time of the continuous phase that increases by orders of magnitude for polymers as opposed to monomeric solvent. Other changes that occur are the length scales over which effects are felt, which in the case of polymers could be over the length represented by the radius of gyration for polymers when not subjected to external forces such as shear. These changes however can be accounted for to give accurate models that describe particle-polymer systems.

PRISM

The Polymer Reference Interactive Site Model or PRISM, is an integral equation theory that builds the theory of particles suspended in polymers taking into account the first-order interactions between polymer segments and the particle surface to describe the degree of particle dispersion and structure of the filled polymer melt. It has its origins in the theory of monatomic liquids[15]. This was later generalized by Chandler and Andersen to extend it to molecular fluids and thus called Reference Interactive Site Model or RISM. Schweizer and Curro extended this theory further in order to apply it to particles in polymer melts which led to the development of PRISM[15].

PRISM has been developed to determine polymer segment and particle microstructures and the energy of the entire system. As a result, it will describe phase separation into particle rich and particle poor phases under conditions where this is the lowest free energy of the system. A key prediction of PRISM is that for hard spheres suspended in a polymer whose segments experience no enthalpy of adsorption in being moved from the bulk to the particle surface will phase separate. This phase separation is driven by the excluded volume of the particles that raises the energy of the composite material while separating particle sand polymer gives rise to greater volume for the polymer segments and thus lowers the composite free energy. This is an entropic phenomena and has direct links to depletion force studied in dilute suspensions to which non-adsorbing polymer is added. Under these depletion attraction conditions, the particles can remain dispersed, phase separate, crystallize or form gels, which depends on the size and concentration of the polymers[15].

Introduction of weak attractions between the particles and polymer segments results in more complex phenomena such as the binding of an adsorbed layer of polymer to the particle surface, which acts as a steric repulsive barrier thus preventing particle aggregation. The polymers can also create bridging between particles, where the same polymer chain is bound to more than one particle. In cases where the particle and the polymer are not index-matched, van-der-waals forces can also cause phase separation, crystallization or gelation[16].

TWO BODY INTERACTIONS

Hooper and Schweizer[16] studied the effects of parameters in PRISM on the stability of polymer nanocompsoites. Parameters of importance are: diameter of the particle, D, the polymer's degree of polymerization,N, the polymer segment diameter,d,, as well as the spatial range, α, and magnitude of polymer-particle and particle-particle interactions, ε_{pc}. These are parameters that in a practical application can be controlled and tailored due to being a function of material properties. It was found that the ratio D/d, is the important parameter rather than the radius of gyration Rg of the polymer, in determining the absolute magnitude of the potential of mean force, Wcc(r) ,relative to the thermal energy, kT. It was also observed that the attractive aspects of the phenomena acted independently of the size asymmetry aspects and thus one can predict trends based solely on the variation of ε_{pc} and α, while holding the size ratios constant. The absolute magnitude of the potential of mean force Wcc(r) would however depend upon the size asymmetry.

Upon varying the attractive forces, four states of the model two-particle system were found to occur which included contact aggregation due to depletion, steric stabilization, local bridging, and longer-range tele-bridging attractions. The particle volume fraction ranges where these states are observed are predicted to change with, α and ε_{pc}. The results are insensitive to degree of polymerization and the exploration of parameter space was limited to particle to monomer diameter ratios above 4-6. The extent of polymerization does not qualitatively change the results.

To summarize, at very low values of ε_{pc}, the particles behave like as in an athermal system where they are contact aggregated due to large depletion attractions. As ε_{pc} increases, the polymer chains form a stable adsorbed layer on the surface, which provides steric stabilization, and results in thermodynamically stable dispersions of particles in the melt. As ε_{pc} further increases, at low and moderate α, the particles are bridged at a particle surface-to-surface separation of n*d, where n is a function of α which is usually from 1-4. At higher values of α, the particles, already sterically stabilized by the polymer chains, undergo bridging attractions over a longer range or so called tele-bridging.

MANY BODY INTERACTIONS

Schweizer and Hall[17] built upon the work described above to extend the concept to many body interactions in composite melts, where the relationships between the polymer-particle attractions ε_{pc}, the volume fraction ϕ of the particles and the pair distribution of the particles in the melt g(r). The advances made by the authors in computational techniques allowed them to solve coupled non-linear integral equations using much more efficient numerical algorithms. This allowed for the study of polymer nano-composites at high filler volume fractions, which was previously restricted to cases of two-body interactions. Using computational techniques developed, full spinodal curves covering from dilute filler to dilute polymer volume fraction regimes were constructed and critical points identified. Thus, phase diagrams for filler-polymer melts could be constructed which would elucidate the different phases of the polymer nano-composite as a function of the polymer-particle interaction ε_{pc}, the filler packing volume fraction ϕ, the spatial range of attraction α, the particle diameter D, monomer diameter d, and the degree of polymerization N.

The phase diagram reiterates the earlier studies showing that at low ε_{pc}, depletion forces result in contact aggregation over a large range of ϕ. At moderate values of ε_{pc} the polymer chains adsorb on the filler particles creating a layer that sterically stabilizes the particles while moving into a region of high ε_{pc}, bridging occurs. The phase boundaries are weak functions of ϕ.The range of the miscibility window is shown to be largely unaffected by the D/d ratio and degree of polymerization. An important result of the study is that as α decreases, the ε_{pc} required to cross over from depletion to the miscibility zone becomes greater and greater. The reason for this is that at the same strength of contact aggregation, the interfacial cohesion is weaker for shorter-range attractions. The mathematical techniques developed in this study also allow for the study of real and Fourier space structure of the polymer nano-composites.

EXPERIMENTAL VERIFICATION OF PRISM

Studies done by Hall and Anderson[18] were able build upon the theories presented by the studies above and quantitatively confirm the results using a experimental model system composed of 44 nm Stober process silica particles that were suspended in polymer melts of PEG and PTHF. The idea was to vary the interaction potential ε_{pc} values between the silica particles and the polymers by changing the chemistry of the polymers. The structure factors were obtained for the composites of varying filler volume fraction ϕ by x-ray scattering (SAXS) by dividing the concentrated particle scattering intensity by the dilute particle limit scattering. The structure factors were also calculated from first order principles using PRISM for comparison over a range of ε_{pc}. The ε_{pc} values were then optimized (by eye) to match the structure factors obtained from theory and experiment for PEO and PTHF based composites.

The three main features of the composite structure factors, the intensity, the position of the peak, and the inverse osmotic compressibility, were compared and found to be in good agreement for the optimized values of ε_{pc}. The ε_{pc} values reported for PEO was 0.55 kT and 0.35 kT for PTHF. It was also noticed that there was a slight upturn with the collective structure factor obtained experimentally for PTHF suggesting that it may be nearing the boundary for phase separation, which was also corroborated by the spinodal diagram. Thus the PRISM theory and experimental model system seemed to agree quite well on many different aspects. The authors suggest a simple model for explaining the difference in ε_{pc} values between PEO and PTHF. The interaction potential is assumed to originate from the hydrogen bonding between the surface hydroxyl groups of the silica and the oxygen in the polymer backbone. Since PTHF has 60% of the oxygen content of PEO per weight, multiplying 0.55*0.6 gives a value of 0.35, which is in good agreement with what is observed. The change in the degree of polymerization N in PEO does not seem to affect the calculated value of ε_{pc} for PEO at 0.55 and the data for PEO400 and PEO1000 seem to coincide and that is predicted by PRISM. Thus PRISM theories are found to work well in practice.

PRISM PREDICTIONS FOR TETHERED PARTICLES

Jayaraman and Schweizer[19] generalized a form of PRISM to study the structure and phase behavior of tethered nanoparticles in a homopolymer matrix. In the absence of a polymer matrix, the tethered nanoparticles were found to exhibit strong concentration fluctuations that indicated an aggregation or microphase separation phenomenon. In the presence of a dense homopolymer matrix, there seemed to be competition between the tether-mediated steric stabilization leading to microphase separation and the polymer matrix induced depletion-like attraction which led to macrophase separation.

The role of the tether length, particle size, number and placement of tethers, total packing fraction and interparticle attraction strength on the structure of the dispersion were studied along with the aggregation and microphase separation behavior. It was found that by increasing particle volume fraction and/or nanoparticle attractions, that strong concentration fluctuations, that indicated microphase separation was occurring. The microphase separation spinodal temperature was found to be a non-monotonic function of the polymer matrix chain length. The increasing size of the nanoparticle keeping the same tether length increased the tendency for macrophase separation. If the size of the particle and the tether length were increased keeping the volume occupied by the particle and the tether monomers the same, the spinodal temperature remained constant although the effect of varying the polymer matrix chain length decreases. This is explained due to the fact that as the size of the particle increased compared to the tethers (or the size of the tethers got smaller compared to the particle), the shielding of the particle core is not as effective thus favoring macrophase separation. The presence of a homopolymer matrix would then add entropic depletion like attractions to further enhance the macrophase separation. The increase in the number of tethers caused the microphase spinodal curves to become more dilution-like due to enhanced steric stabilization from the increased tethers, and the role of polymer matrix chain length, tether length and particle size on the spinodal temperature decreased.

SUB-EINSTEINIAN RHEOLOGY OF NANOCOMPOSITES

As covered in the above section on colloids, it is expected that as particles are loaded in either a low molecular solvent or polymer melt, according to Einstein[5], the effective viscosity of the dispersion for hard spheres in the low volume fraction limit increases as :

$$\eta_{eff} = \eta_s (1 + 2.5\Phi)$$

where η_s is the solvent viscosity and Φ is the volume fraction of particles in the suspension. The equation may also be written as:

$$(\eta_{eff} - \eta_s) / \eta_s = [\eta]\Phi$$

where for the above limiting case as described, $[\eta]$ which is also known as the intrinsic viscosity which equals 2.5 for hard spheres. This has been experimentally proven again and again. This relation is independent of particle size. Batchelor[6] improved upon this model to correct for effects resulting from attractive repulsive forces to give :

$$\eta_{rel} = \eta_{eff} / \eta_s = 1 + 2.5\,\Phi + 6.2\,\Phi^2$$

where η_{rel} is the *relative viscosity*. The equation above may also be written as :

$$(\eta_{rel} - 1) / \Phi = 2.5 + k_H\,\Phi$$

where the left hand side of the equation is also known as *reduced viscosity* and k_H is known as the Huggin's coefficient[13]. In case of Batchelor's model that only takes into account the hydrodynamic and Brownian interactions, k_H = 6.2, where of that, 2.5 is from near-field hydrodynamic interactions, 2.7 from far-field hydrodynamic interactions and 1 from Brownian motion.

In recent years, research has increasingly focused on composites of nano-materials. The extremely high surface area to volume ratios and sizes that are comparable to the segment size of the particles gives rise to new regime of physics that can cause the rise of unusual effects that are not predicted by classical colloidal theory. One of them is the effect that particle size can have on rheology of polymer melts, which will be the focus of this thesis.

Tuteja and Mackay[4] that nanoparticles of polystyrene in a polystyrene homopolymer matrix that were above the entanglement molecular weight (above which the viscosity scales with approximately 3.4-3.8 power as opposed to 1), caused a significant decrease in viscosity. Since the dispersion was homogenous ideal blend, no enthalpic interactions between the particles and the polymer matrix chains were expected simplifying the model experimental system. This

therefore helped isolate the effects that particle size had on entanglements and viscosity. This effect was found only to be specific to polymers above their entanglement molecular weight. Below the entanglement concentration an increase in viscosity was observed with the same particles. The particles were characterized as soft Gaussian spheres using small angle neutron scattering (SANS). The spheres were made using polystyrene chains of different molecular weights having crosslinking sites at regular intervals on the polymer backbone that helped crosslink the polymer chain into its particle configuration.

In the study[4], it is hypothesized that when the interparticle half gap (h), twice the distance of which is the distance of separation between two particles, becomes less than the radius of gyration of the matrix polymer chain, the chains experience confinement wherein they are forced to disentangle and configure themselves in a stretched manner so as to fit in between the particle surfaces. Viscosity of less than half the original viscosity is seen.

Kopesky et al[20] observed similar phenomenon with polyhedral oligomeric silsequioxane particles (POSS) dispersed in a polymethyl methacrylate polymer matrix. The POSS particles were soluble upto 0.05 percent volume fraction after which they existed in an aggregated crystallite form. The POSS particles were mostly dispersed in a nanoscopic manner, which was confirmed through x-ray scattering studies. Remarkably, there was a viscosity reduction observed even though no lowering of glass transition temperature was seen. Therefore there was a decrease in viscosity from a mechanism that did not involve an addition of free volume with the addition of POSS particles. The addition of isobutyl and cyclohexyl POSS particles caused initial downturns in viscosities before moving upwards at concentrations higher than the solubility limit at which point the aggregates tended to follow classical predictions for rheology of hard sphere filled suspensions. The viscosity drop caused by the isobutylPOSS was seen to be of a slightly higher magnitude compared to the cyclohexylPOSS.

Kim and Zukoski[21] conducted studies on a model experimental system of silica particles (44 nm) in different polymers in order to vary the polymer segment-surface interaction potential ε_{pc}. The particles were much larger than the polymer segment and considered model hard spheres. The viscosity of the system was modeled after the classical colloidal theories given by Einstein and subsequently corrected for interaction potentials by Batchelor[5,6] :

$$\eta_{rel} = \eta_{eff} / \eta_s = 1 + 2.5k\,\Phi + 6.2\,\Phi^2$$

where k represents how the adsorbed polymer layer influences viscosity. With an adsorbed layer, the hydrodynamic diameter is expected to increase and thus would result in a larger viscosity increase for the same particle volume fraction since the hydrodynamic volume fraction $\phi_\eta = \phi k$ is larger than the actual particle volume fraction. Anderson and Zukoski[22] showed that, although k varies with Rg of the polymer as expected, the zero shear rate viscosity vs hydrodynamic volume fraction curves collapsed to a single fit.

The study by Kim et al[21] compares the ε_{pc} values of silica particles dispersed in polymer melts of various chemical structures to values of k determined for the same dispersions to find a monotonic relationship between the two at the same matrix polymer molecular weight. As ε_{pc} is lowered, it is found that k decreases as well in a linear fashion from k>1 for ε_{pc} values of 0.55kT to k=0.25 for values of 0.15kT.

Kim et al[21] conclude that as the ε_{pc} values drop, there seems to be an increase in the slip length of the polymer chain over the particle surface is the reason for viscosities that are lower in value than expected. It is also confirmed through PRISM predictions of the particle polymer segment density fluctuations that as ε_{pc} is reduced there is a depletion of polymer at the surface of the particle that may be giving rise to lower viscosities. The authors caution against extrapolating the data of k vs ε_{pc} to negative intrinsic viscosities because this phenomenon as discussed in the preceding section is associated with particles that are approaching the diameter of the polymer tube radius, the polymer being above the entanglement molecular weight and the interparticle gap being smaller than the radius of gyration of the polymer. Another reason is that if the ε_{pc} is dropped below 0.15kT, the particles will phase separate due to strong depletion forces whereas in the case of systems where negative intrinsic viscosities are seen, the particles are well dispersed.

Negative intrinsic viscosities are not limited to systems with high molecular weights such as polymers as seen in studies by Striegel and Alward[23], using a binary system comprising of low molecular weight polyethylene oligomers dissolved in a solution of N,N'-diacetylamide/LiCl.

CHAPTER 2: EXPERIMENTS & DATA ANALYSIS

POLYHEDRAL OLIGOMERIC SILSESQUIOXANE (POSS)

Polyhedral oligomeric silsesquioxane or POSS particles are cage like structures containing a siloxane backbone consisting of silicon and oxygen atoms. The cages generally tend to be cubic although a small proportion of them may be of higher order. The cage-like structure of the POSS particle/molecule has the silicon atoms at the corners and the oxygen atoms along the edge joining each silicon atom to the other as illustrated below :

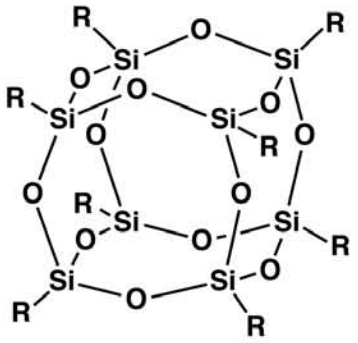

Fig 1. Cubic cage structure of POSS with R representing organofunctional moieties

The R groups are pendant on the corners of the eight Si atoms and can be varied to almost any possible functionality. Functionalities can vary for example from PEG chains and alky chains to reactive moieties such as vinyl, mercapto, carboxylic, imido as well as ionic groups such as sulfonates and quaternary ammonium ions[24]. Therefore POSS molecules may find many applications in composites as a nanophase material due to the flexibility in tailoring it for the specific application. The POSS molecules have been known to alter properties of polymers in novel ways when incorporated in polymer melts either in a untethered form or as a pendant group hanging off the polymer backbone.

The focus of the thesis is on the rheology properties imparted by incorporating POSS molecules with polyethylene glycol pendant chains in a polyethylene glycol homopolymer melt. Similar studies are done incorporating POSS molecules with isooctyl and isobutyl pendant groups in polydimethylsiloxane polymer melt.

CHARACTERIZATION OF POSS DIAMETER

POSS molecule sizes in solution were characterized using small angle x-ray scattering techniques at Argonne national lab beamline 5-ID and viscosity was measured using a Bohlin controlled stress BCS 2:4 type rheometer with a 4 degree 40 mm cone and plate setup.

Small angle x-ray scattering experiments were performed at Argonne national lab beamline 5-ID using x-rays at 17 eV to gather information in q-wave vector range from 0.04 to 0.27 A^{-1}. Using the data we use Zimm analysis to extrapolate the radius of gyration Rg for the systems of PEGPOSS in Ethanol (POSS particles with eight polyethylene oxide chains of MW ~ 600 tethered to the Si atoms), IsooctylPOSS in hexane (R = Isooctyl chains) and PEGPOSS in water. The diameter for the PEGPOSS in Ethanol was estimated to be 2.37 nm and 2.57 nm in water. This could be due to different swelling of PEG chains in ethanol as opposed to water. The diameter for IsooctylPOSS in hexane was estimated to be 2.56 nm. The method of extrapolation was as follows:

$$I(q,c) = (c/m)*P(q,c)*S(q,c) = (c/m)*[1-(5/9)(D/2)^2*q^2]/[1+2A_2*c]$$

where I(q,c) is the net scattering from the sample, c is the concentration of the sample in g/ml, m a constant that contains information about contrast, D the diameter of the POSS particle, q being the wave vector which is $4\pi/\lambda*\sin(\theta/2)$ where λ is the wavelength of the x-rays. A_2 is the second virial coefficient. This is the standard equation for Zimm analysis[25]. The Zimm analysis is only valid in the limit where $q \rightarrow 0$ and $c \rightarrow 0$. This equation thus, simplifies to:

$$c/I(q,c) \sim m*[1 + (5/9)(D/2)^2*q^2][1+2*A_2*c]$$

First we plot c/I(q,c) versus q^2 for different c as illustrated in Fig 2. below:

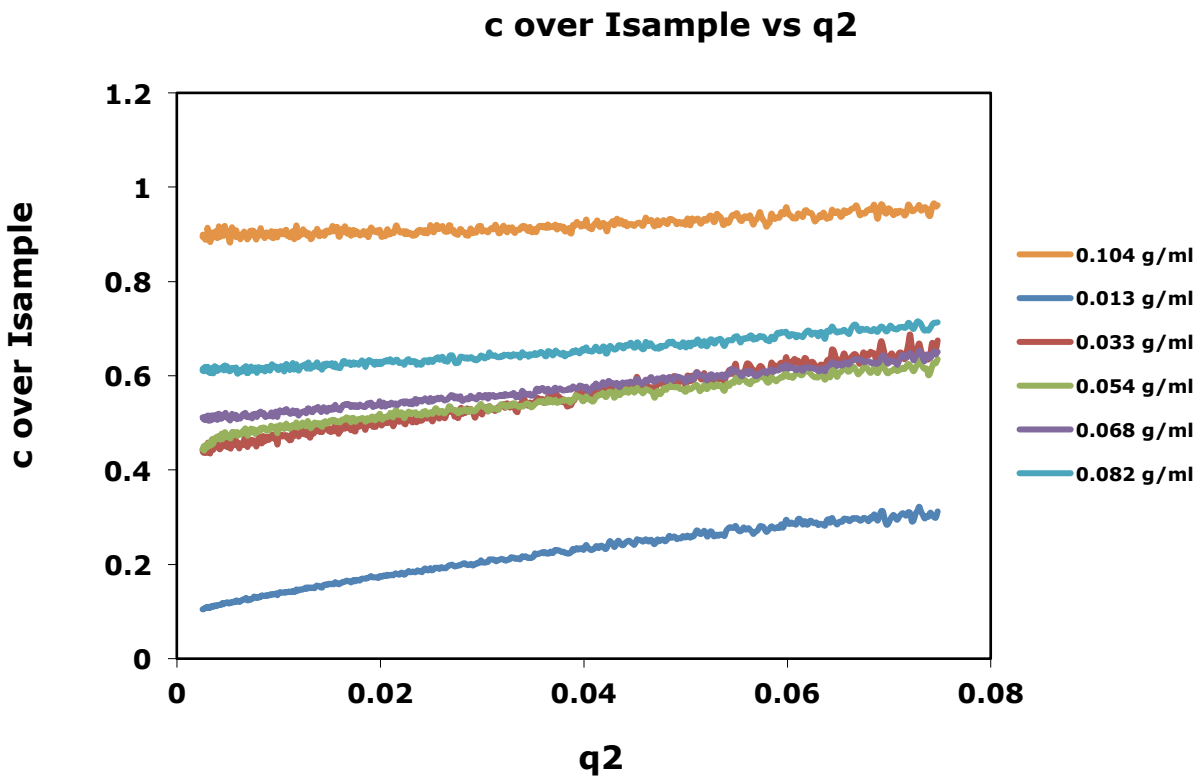

Fig 2. c/I(q,c) versus q^2 (A^{-2}) for Isoctyl POSS in Hexane at different weight percentages

We get a fit on the data in the form of a line a'(c) + b'(c) * q^2 with a'(c) = m[1+2A_2] and b'(c) = m[(5/9)(D/2)^2][1+2A_2c]. Plotting a'(c) versus c yields a line of intercept m and slope m*2A_2 as illustrated in Fig 3. below:

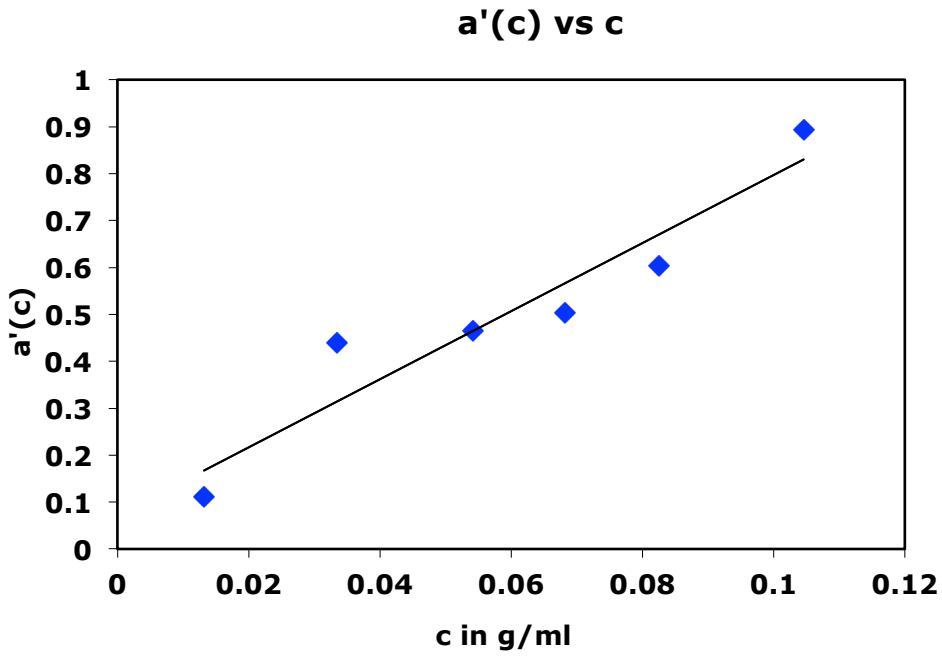

Fig 3. a'(c) versus c

Thus we can calculate the second virial coefficient A_2. If we choose a range of q values in the limit that q → 0, and plot c/I(q,c) versus c for each q value, we get a data that fits to the form a(q) + b(q)*c where $a(q) = m[1+(5/9)(D/2)^2*q^2]$ and $b(q) = m[1+(5/9)(D/2)^2[2A_2]$ as illustrated below in Fig 4. using fewer q values for sake of better illustration. Plotting a(q) vs q^2 (as show in Fig 5.) thus allows us to calculate D from the slope:

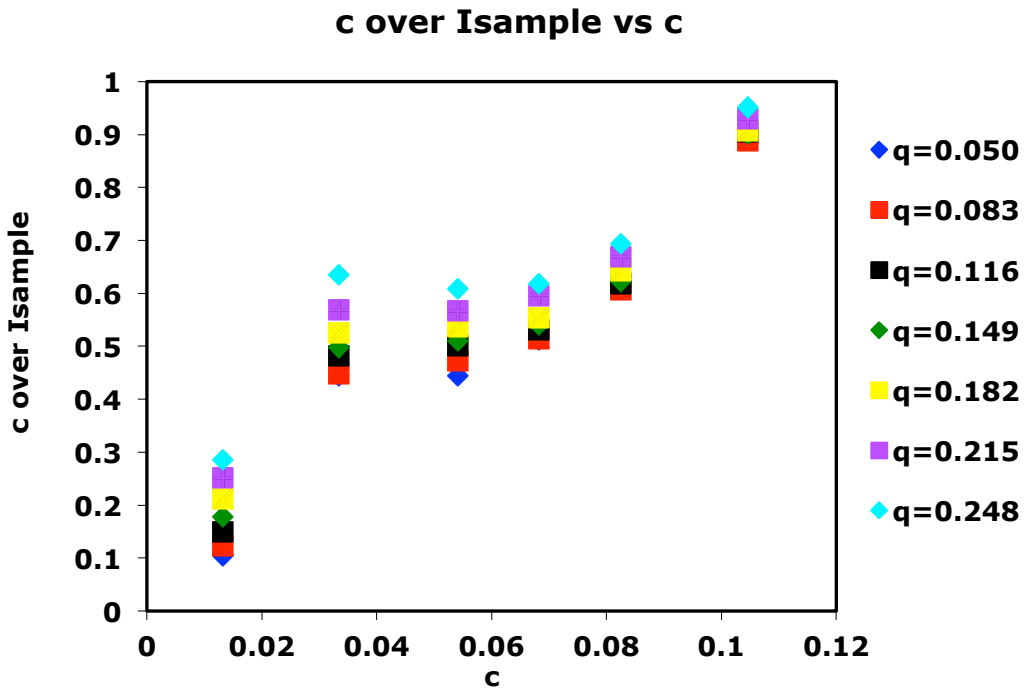

Fig 4. c/I(q,c) vs c for different q (A^{-1}) values.

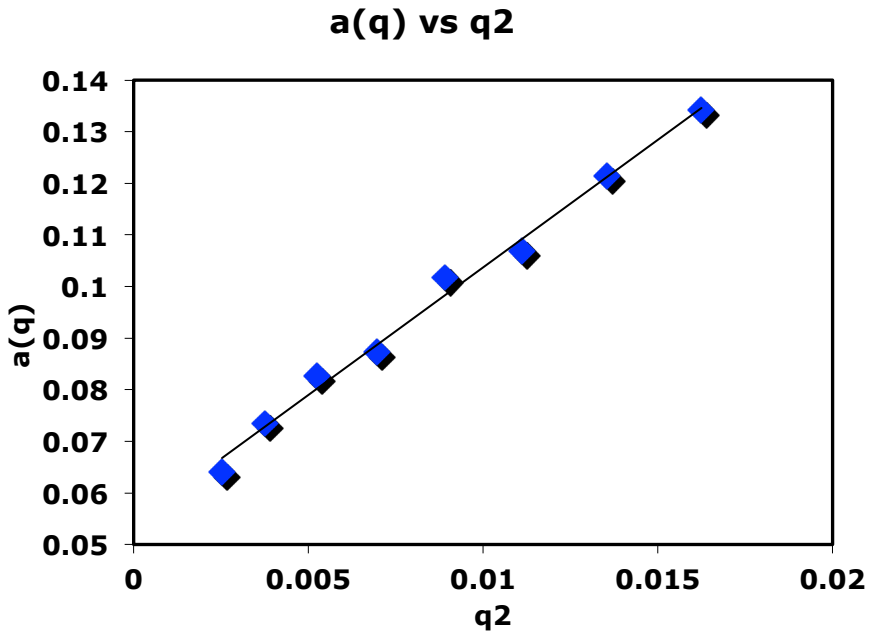

Fig 5. a(q) vs q^2 (A^{-2}).

Thus plotting a(q) versus q^2 gives an intercept of m and a slope of $m[(5/9)(D/2)^2$. Thus we can calculate D. Table 1 below summarizes D of POSS particles dissolved in solvent for various systems along with A_2, the second virial coefficient :

System	D (nm)	A_2
PEGPOSS in Ethanol	2.4	3.0
PEGPOSS in Water	2.6	14.8
IsooctylPOSS in Hexane	2.6	50.7

Table 1: D, A_2 of POSS in various systems calculated using Zimm analysis

To countercheck the validity of the Zimm analysis, the intrinsic viscosity of PEGPOSS in ethanol as a function of PEGPOSS volume fraction was plotted. The slope was found to be 1.5. The data is illustrated below in Fig 6 :

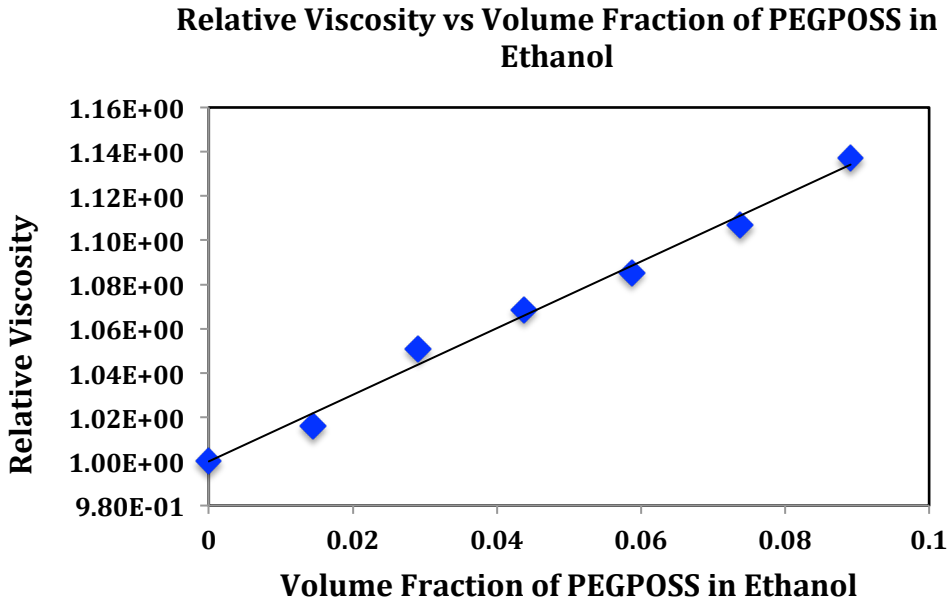

Fig 6. Relative Viscosity vs Volume Fraction of PEGPOSS in Ethanol

The data was fitted using the classical relative viscosity prediction by Einstein for low volume fractions, $\eta_{rel} = 1 + 2.5k\phi$. Thus $k = 1.5/2.5 = 0.6$. Thus, the hydrodynamic volume $\phi_d = k\phi = 0.6\phi$. Thus the apparent density of PEGPOSS = 1.1/0.6 = 1.83 g/ml where 1.1 is the density of PEGPOSS in g/ml which was measured using a densitometer. Thus using the apparent density of 1.83 g/ml of PEGPOSS and a molecular weight of approximately 7000[24], and assuming a roughly spherical shape, the diameter of PEGPOSS was calculated to be 2.3 nm. This is in comfortable agreement with the diameter calculated using X-ray scattering of 2.4 nm. The slight discrepancy of 0.1 nm could have risen from the fact that the diameters are calculated on different principles in the two techniques. While the viscosity measurement calculates the hydrodynamic diameter, the Zimm analysis calculates the diameter based on the scattering length density that is based on the distribution of mass of the particle around the center. Another reason for the discrepancy could be the fact that the molecular weight of the PEGPOSS is not exactly 7000 since the POSS cage is only approximately 8 Si atoms and can range upto 12 Si atoms in relatively small quantities, but enough to raise the average molecular weight and thus skew the data. Thus Zimm analysis results are assumed reliable.

PEGPOSS / PEG MIXTURES: EFFECT ON MELTING TEMPERATURE

Differential Scanning Calorimetry was carried out on PEGPOSS / PEG4000 mixtures of sample size 1 milligram at a ramp rate of 5 degrees C per minute, to determine if any unusual changes in the crystallization or melting behavior occurred as a result of the present of PEGPOSS in the PEG 4000 polymer. The results are shown below in Fig 7a:

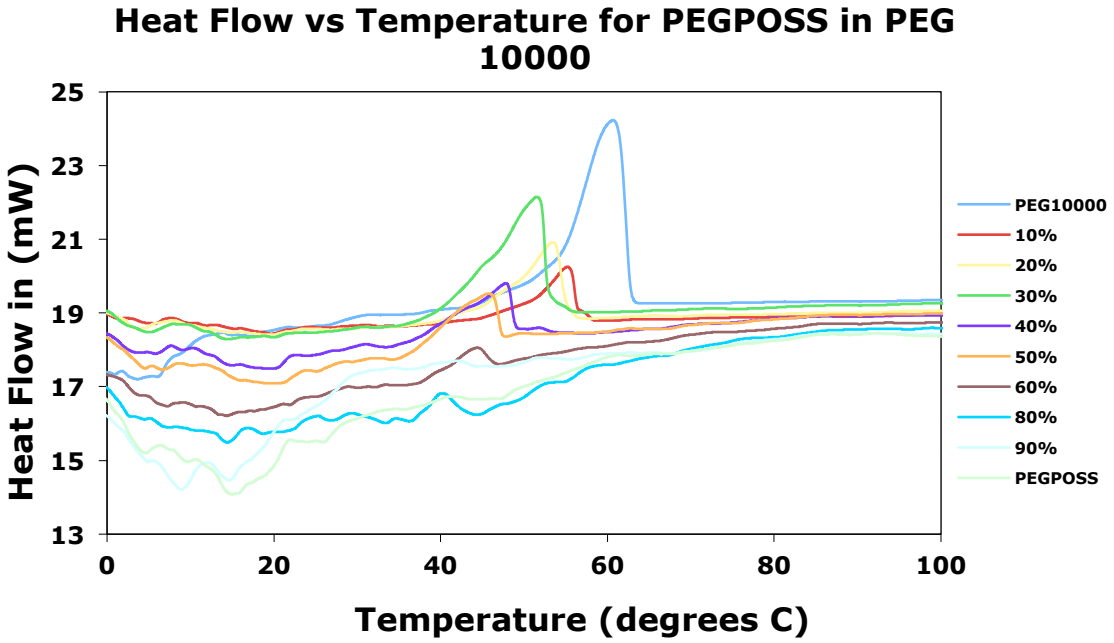

Fig 7a. Heat Flow into (endo) the sample in mW versus temperature in degrees C for different compositions of PEGPOSS in PEG 10000

The temperature of the melting peak was observed for each composition and plotted as a function of percentage by weight of PEGPOSS. The crystallization peak of PEG 10000 is seen at roughtly 60 degrees C which has been reported in literature[26]. The melting temperature was show to vary linearly with percentage of PEGPOSS in the composition and eventually disappeared to represent pure PEGPOSS which is a liquid at room temperature. The plot is show below in Fig 7b:

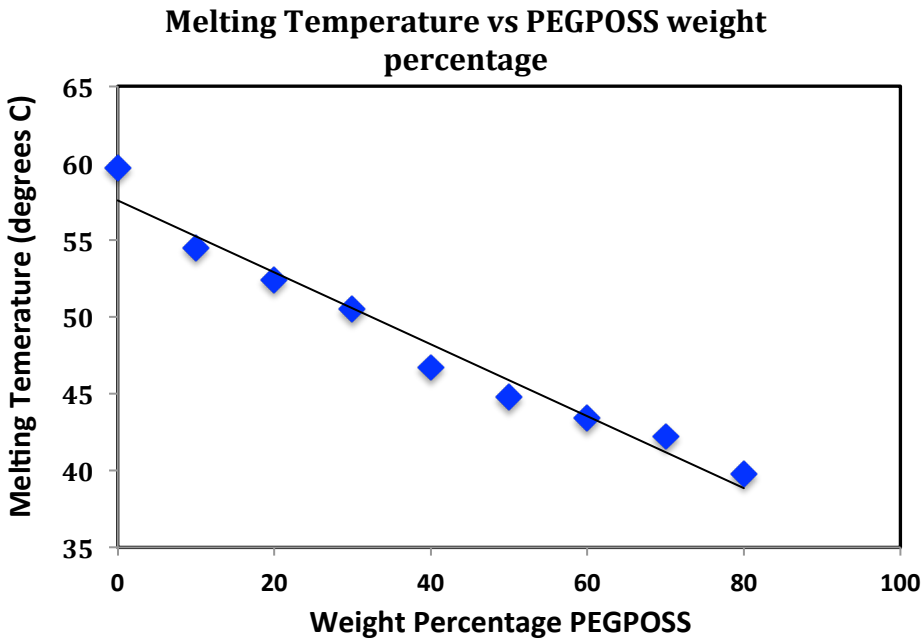

Fig 7b. Melting temperature versus composition of different PEGPOSS in PEG 10000 mixtures.

The melting temperature of the PEGPOSS in PEG 10000 composition was found to decrease roughly linearly with increasing percentage by weight of PEGPOSS in the mixture, which is not surprising since PEGPOSS has a substantially lower melting temperature than PEG 10000. The plot is quite linear and exhibits that the melting temperature changes as a linear function of the amount of PEGPOSS by weight in PEG without any deviations due to binary mixing effects, from 0 to 80 percent.

INTRINSIC VISCOSITY OF POSS-POLYMER MELTS

The viscosity of PEGPOSS in PEG polymers of different molecular weights covering above and below the entanglement regime[27] (diethylene glycol, 400, 600, 4000, 10000) was measured using a Bohlin controlled stress BCS 2:4 type rheometer with a 4 degree 40 mm cone and plate setup. Similarly, IsooctylPOSS and ButylPOSS were dispersed in polydimethylsiloxane (PDMS) polymers of different molecular weight covering above and below the entanglement regime[28] (6000, 17000, 28000 and 63000). For PEGPOSS in PEG

mixtures, PEGPOSS, which is a liquid at room temperature, was simply dissolved in melted PEG above 70 degrees and stirred in a 20ml vial vigorously using a Thermodyne Maxi Mix II vial mixer. The resulting melts were made for various volume fractions of PEGPOSS in PEG at each molecular weight of PEG and were found to be transparent with no phase separation present. The PEGPOSS/PEG melt sample viscosities were then measured at different volume fraction loadings at a temperature of 76.5 +/- 0.1 °C since a high enough temperature was required to ensure that the higher molecular weight PEGs were melts. The relative viscosity of the melts versus volume fraction of PEGPOSS was then plotted as shown in Fig 8. below:

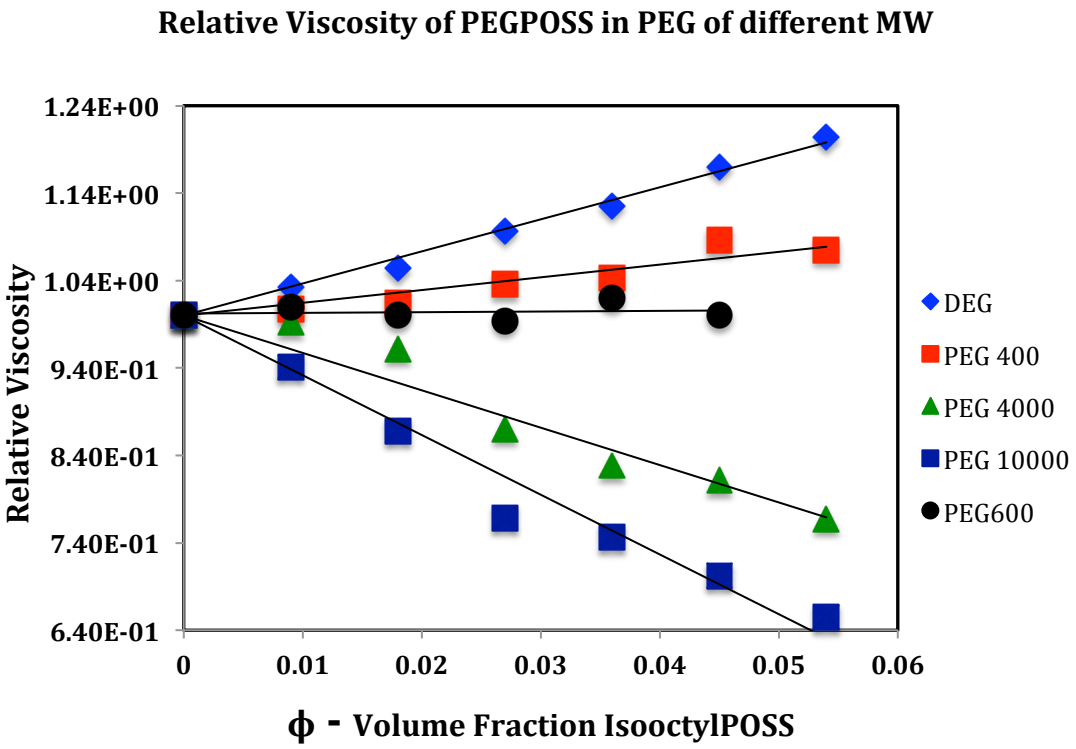

Fig 8. Relative Viscosity of PEGPOSS in PEG of different molecular weights (diethylene glycol, 400, 600, 4000, 10000).

The PEGPOSS viscosity itself was measured to be $2.75*10^{-2}$ Pa.s. The viscosities of the different PEGs used is given below in Table 2:

PEG molecular weight	Intrinsic Viscosity	Viscosity in Pa.s
DEG (PEG dimer)	3.66 ± 0.16	5.59E-03
400	1.45 ± 0.22	1.40E-02
600	0.0762 ± 0.27	2.07E-02
4000	4.27 ± 0.48	2.62E-01
10000	6.83 ± 0.53	2.72E+00

Table 2. Absolute Viscosities in Pa.s of different molecular weights of Polyethylene Glycols

The IsooctylPOSS, which is a liquid at room temperature, was directly mixed into the PDMS and stirred vigorously like in the case of PEGPOSS and PEG composites and found to be transparent with no phase separation below 20 percent by weight. Above 20 percent phase separation was visibly present regardless of molecular weight. The IsobutylPOSS, which is in the form of the white powder at room temperature, was first dissolved in warm hexane at a mass fraction of 10 percent after which the transparent solution was added to PDMS polymer and stirred using the vial mixer. The resulting polymer-POSS solution mixture was transparent and placed in a vaccum oven overnight at 25 mmHg below atmospheric pressure at a temperature of approximately 45 degrees C to facilitate the evaporation of hexane. The resultant IsobutylPOSS-PDMS composite was stable and transparent below 1 percent loadings of POSS, but above that white crystalline precipitates could be observed at all molecular weights, leadings us to conclude that 1 percent was the solubility limit for the IsobutylPOSS in PDMS regardless of molecular weight. Thus, for IsooctylPOSS and IsobutylPOSS composites of various weight fractions at different molecular weights of PDMS were prepared. These viscosity of these samples were then measured using a Bohlin controlled stress BCS 2:4 type rheometer with a 4 degree 40 mm cone and plate setup at 25.3 +/- 0.1 degrees C. The relative viscosity versus volume fraction for IsooctylPOSS in PDMS of different molecular weights is shown below in Fig 9 a,b,c,d. :

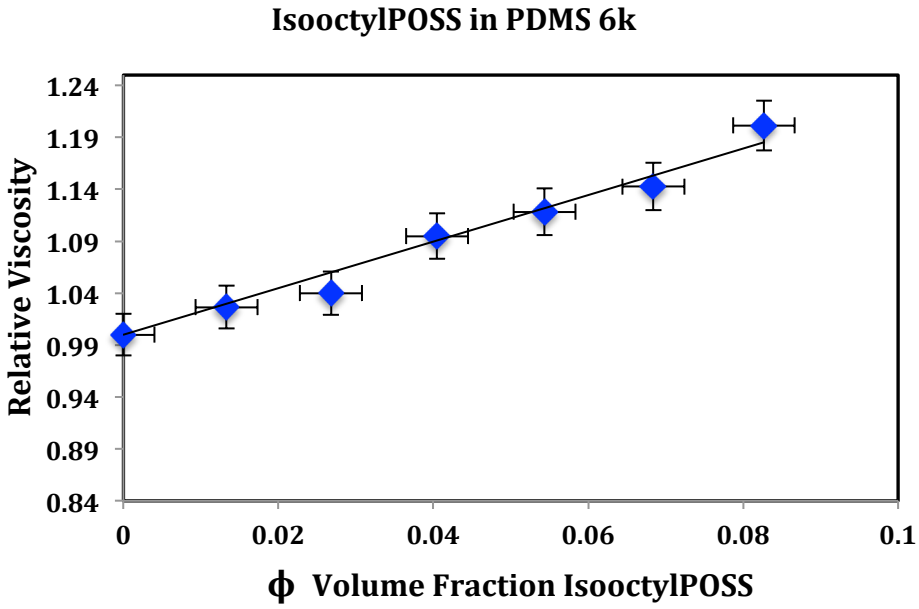

Fig 9a. Relative Viscosity of IsooctylPOSS in PDMS of 6000 molecular weight at different volume fractions.

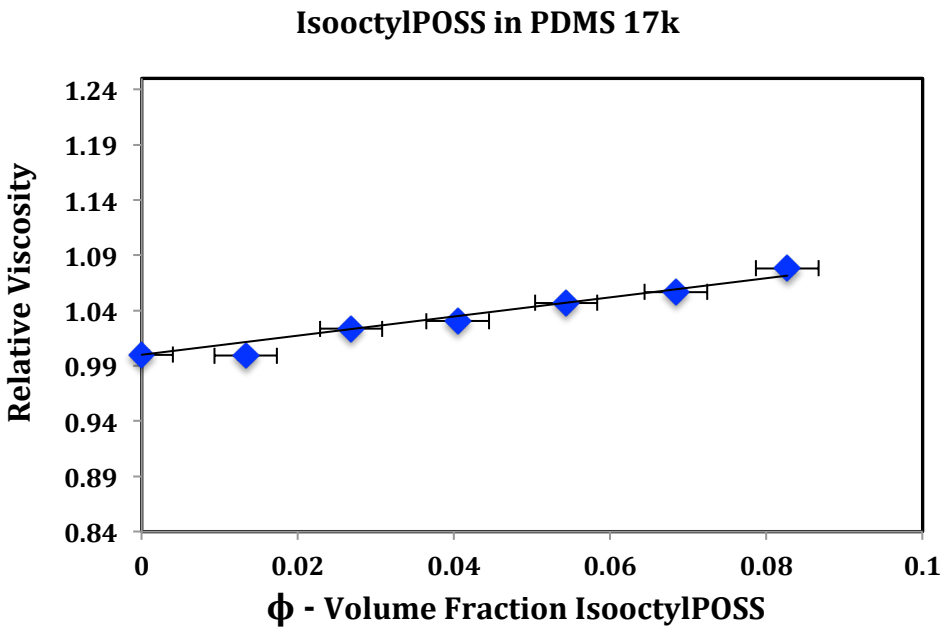

Fig 9b. Relative Viscosity of IsooctylPOSS in PDMS of 17000 molecular weight at different volume fractions.

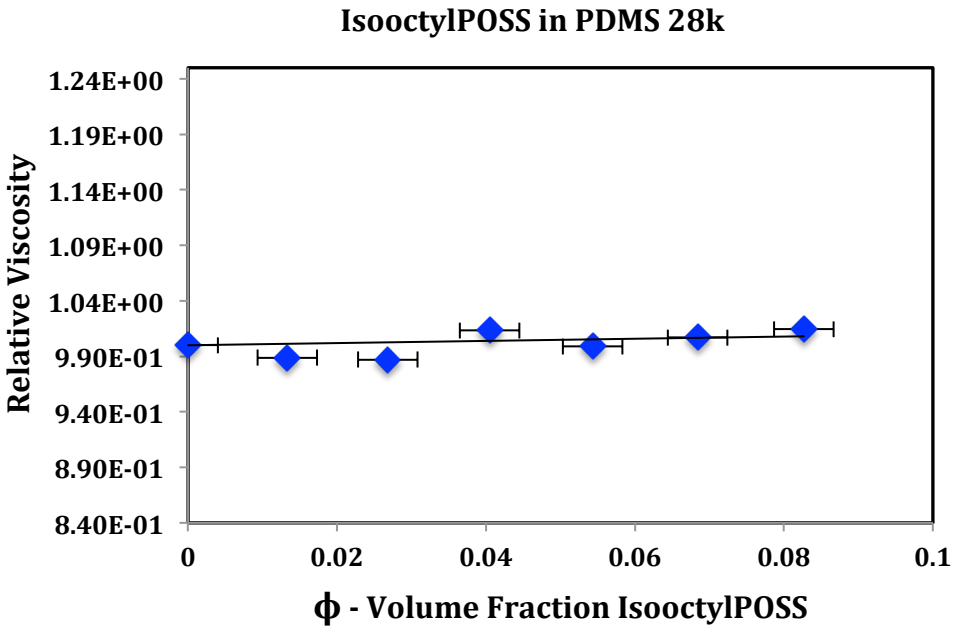

Fig 9c. Relative Viscosity of IsooctylPOSS in PDMS of 28000 molecular weight at different volume fractions.

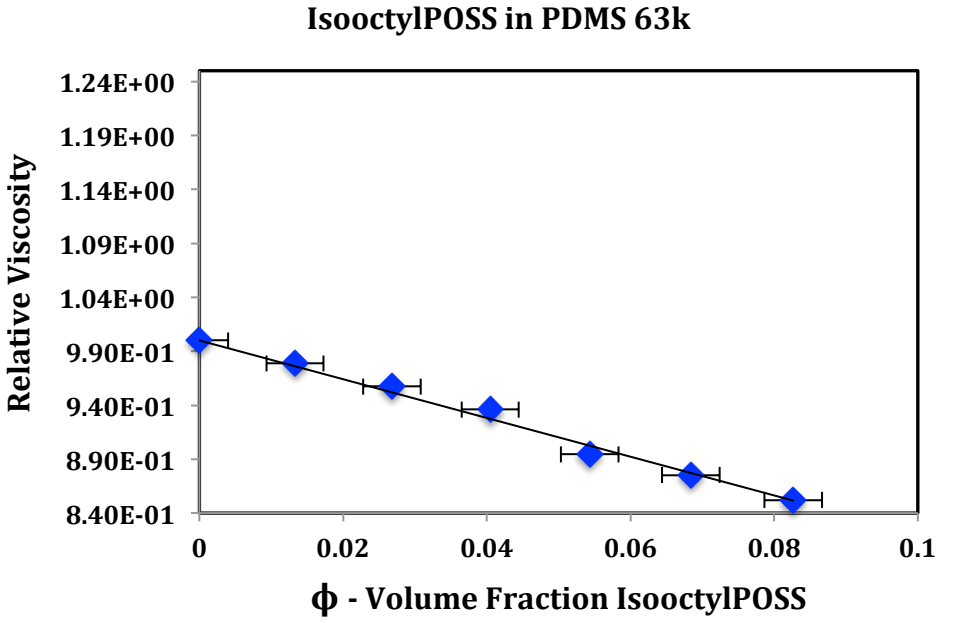

Fig 9d. Relative Viscosity of IsooctylPOSS in PDMS of 63000 molecular weight at different volume fractions.

The slopes of the curves illustrated in Fig. 9a, 9b, 9c, 9d gives us the intrinsic viscosity associated with IsooctylPOSS in PDMS of different molecular weights. The intrinsic viscosities are listed in Table 3 below:

PDMS molecuar weight	Intrinsic Viscosity [η]
6000	2.24 ± 0.25
17000	0.86 ± 0.13
28000	0.1 ± 0.21
63000	-1.79 ± 0.11

Table 3. PDMS molecular weight versus intrinsic viscosity for IsooctylPOSS.

The relative viscosity versus volume fraction for IsobutylPOSS in PDMS of different molecular weights is shown below in Fig 10 a,b,c,d :

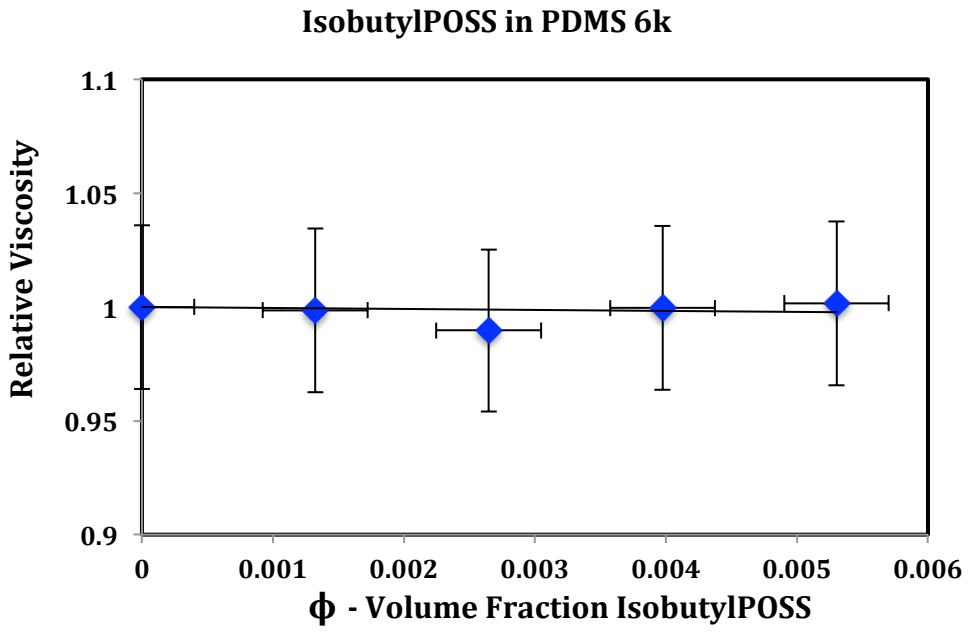

Fig 10a. Relative Viscosity of IsobutylPOSS in PDMS of 6000 molecular weight at different volume fractions.

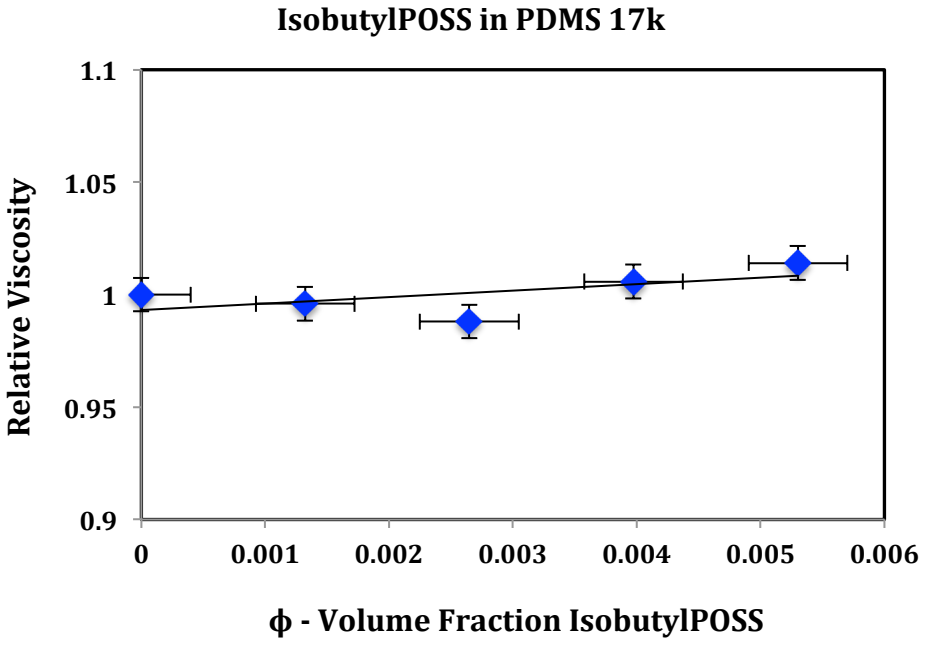

Fig 10b. Relative Viscosity of IsooctylPOSS in PDMS of 17000 molecular weight at different volume fractions.

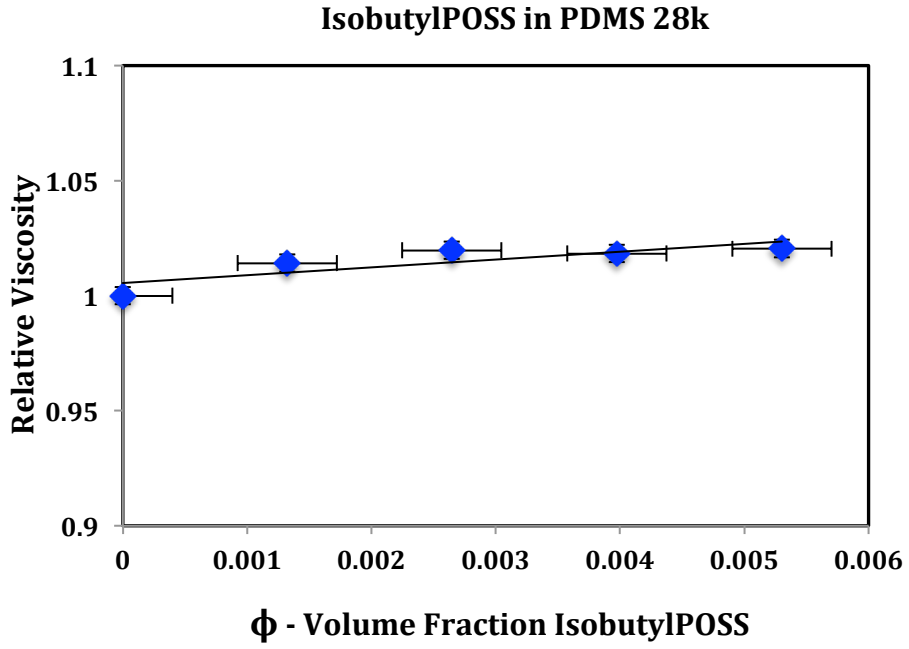

Fig 10c. Relative Viscosity of IsooctylPOSS in PDMS of 28000 molecular weight at different volume fractions.

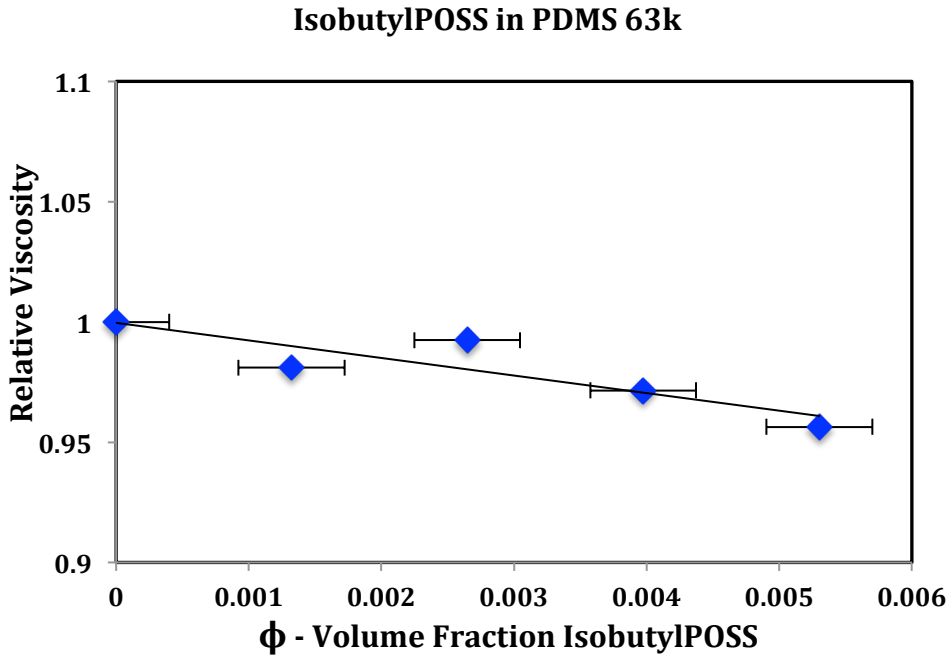

Fig 10d. Relative Viscosity of IsooctylPOSS in PDMS of 63000 molecular weight at different volume fractions.

The slopes of the curves illustrated in Fig. 10a, 10b, 10c, 10d gives us the intrinsic viscosity associated with IsobutylPOSS in PDMS of different molecular weights. The intrinsic viscosities are listed in Table 4 below:

PDMS molecuar weight	Intrinsic Viscosity [η]
6000	-0.43 ± 1.75
17000	2.88 ± 4.13
28000	3.4 ± 2.00
63000	-7.3 ± 3.27

Table 4. PDMS molecular weight versus intrinsic viscosity for IsobutylPOSS

The effect of temperature was studied on the relative viscosity of POSS/Polymer melts. The system of PEGPOSS in 4000 molecular weight PEG was chosen and the viscosity was calculated at two different temperatures of 65 and 75 degrees C. There was no difference to be seen in the relative viscosities at both temperatures as shown in Fig 11 below:

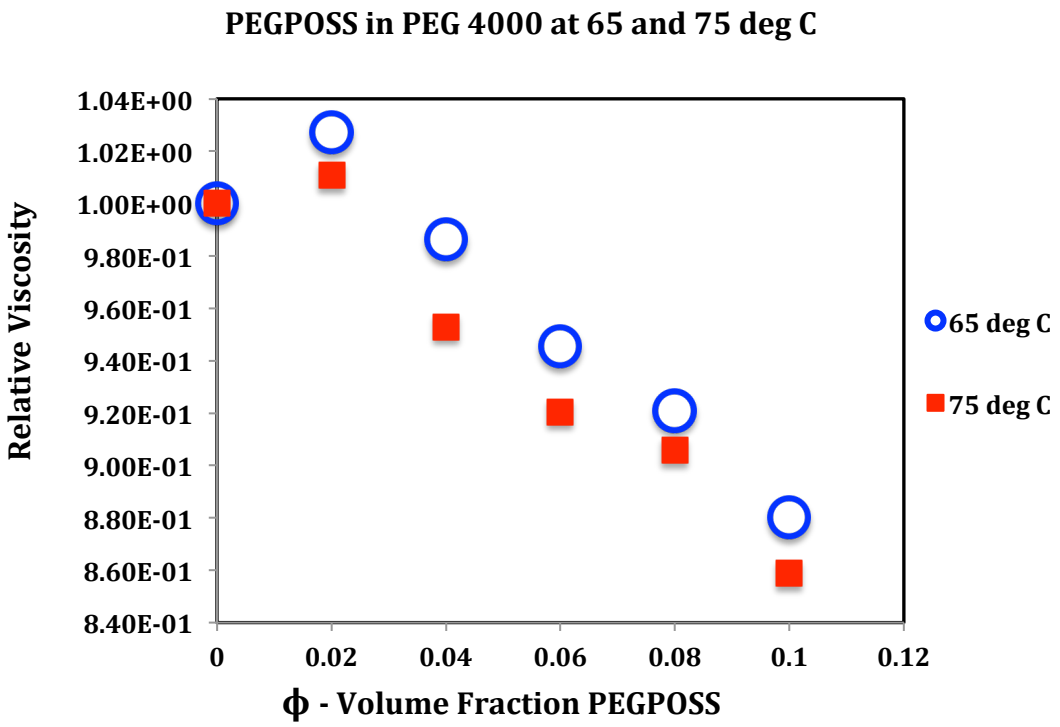

Fig 11. Relative viscosity of PEGPOSS in PEG 4000 at 65 and 75 degrees C.

CHAPTER 3: DISCUSSION AND CONCLUSION

The diameters of the various POSS particles were characterized using small angle x-ray scattering and rheology. The diameters of PEGPOSS in water and ethanol were found to be 2.4 nm and 2.6 nm respectively. The diameter of IsooctylPOSS in hexane was found to be 2.6 nm. The intrinsic viscosity calculated for PEGPOSS in ethanol gives a hydrodynamic radius of 2.3 nm assuming an approximately spherical shape for the POSS particle. This is roughly in agreement with the diameter calculated using Zimm analysis of the x-ray scattering data. The IsobutylPOSS diameter is expected to be approximately the same as the other POSS particles. The interparticle half-gap distance the particles in a polymer melt is described by Mackay et al[4] as shown below:

$$h / a = (\phi_m / \phi)^{1/3} - 1$$

where h is the interparticle half-gap, a is the radius of the particle, ϕ_m is the maximum packing fraction (approximately 0.638 for hard spheres), ϕ is the volume fraction of particles. The interparticle half-gap calculated for the 2.5 nm diameter particles at a volume fraction of 0.001, 0.01 and 0.1 are 9.76 nm, 3.99 nm, 1.31 nm respectively. The radius of gyration of the PDMS of molecular weight 6000, 17000, 28000 and 63000 were calculated to be 1.99 nm, 3.36 nm, 4.31 nm, 6.47 nm respectively calculated using the relationship[29] :

$$Rg = (0.0666*MW^{1.0141})^{1/2}$$

The radius of gyration of the PEG 400, 600, 4000 and 10000 are 4.36 A, 5.34 A, 1.37 nm, and 2.18 nm respectively calculated using the fact that $Rg \sim (MW)^{1/2}$ and that Rg of PEG 600 is 5.34 A[29].

It is observed that for IsooctylPOSS in Fig 5(a,b,c,d) that for PDMS molecular weight of 6000 and 17000, an increase in relative viscosity is seen. The intrinsic viscosity of the mixtures is becoming less as the molecular weight is increased. The intrinsic viscosity is seen to fluctuate over a very small difference in relative viscosity in the 28000 molecular weight PDMS compared to much larger changes as seen in the 6000 and 17000 molecular weight PDMS. Thus, the 28000 molecular weight PDMS data is relatively "flat" compared to the 6000 and 17000 molecular weight data. The fluctuation is probably due to the fact that it is slightly above the point of transition (with intrinsic viscosity of 0.23) where the intrinsic viscosity becomes zero and then becomes negative.

At a molecular weight of 63000, the intrinsic viscosity of the PDMS is negative with respect to PEGPOSS even though the viscosity of IsooctylPOSS is higher than that of the PDMS. This is an unusual result which is not predicted by the classical colloid rheology theories such as the Einsteinian relation for intrinsic viscosity for hard spheres, which would predict a rise, or the theories of simple mixing which would also predict a rise. The pre-condition for negative intrinsic viscosities in systems explored by Mackay et al[4] was that the polymer molecular weight needed to be above the entanglement molecular weight and the interparticle half-gap h be smaller than the Rg of the polymer matrix chain. Clearly the conditions of the $h < Rg$ are not met in the case of IsooctylPOSS dispersed in PDMS but a negative intrinsic viscosity is seen. Thus, the result does not agree with the hypothesis of Mackay et al that the drop in viscosity is attributed to a loss of entanglements. It is however similar to the results as seen by Kopesky et al[20] where they disperse cyclohexyl POSS in PMMA and a downward trend in viscosity is seen before it rises again.

In the case of IsobutylPOSS, the particles are visibly aggregated above 1 percent concentration by weight in the PDMS melt. The reduced tether size compared to IsooctylPOSS dramatically reduces the dispersibility of the particles and in the case of both particles ultimate solubility is not a function of polymer matrix chain length. This is very much in line with PRISM theory predictions for tethered particles as presented by Jayaraman and Schweizer[19]. Thus the intrinsic viscosity data was limited to measurements at concentrations upto 1 percent at increments of 0.2 percent. These are very small amounts being added to the PDMS and thus the potential for errors due to precision are more in this case compared to IsooctylPOSS. The viscosity data fluctuates and shows no clear trend at the lower molecular weight PDMS polymers. At a molecular weight of 63000, a strong drop in absolute viscosity is clearly seen. The result was repeated and verified. The IsobutylPOSS is a white solid amorphous powder at room temperature. The difference in absolute viscosity for the four molecular weights at different IsobutylPOSS levels is shown below in Fig 12:

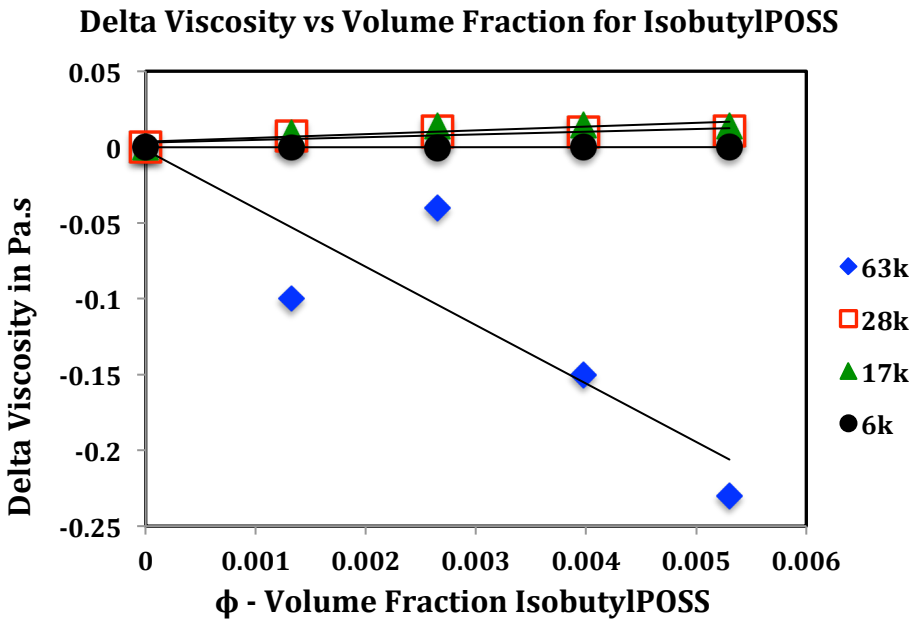

Fig 12. Absolute difference in viscosity versus volume fraction of IsobutylPOSS particles in PDMS of different molecular weights.

Thus we conclude from from Fig 8, that the drop from the very low volume fraction IsobutylPOSS particles dispersed at such low volume fractions is indeed real and substantial. It is again interesting to note that the interparticle gap size h is not less than Rg for IsobutylPOSS at such low volume fractions (0 – 1 percent). Thus the drop in viscosity cannot be attributed to the loss of entanglements in the case of IsobutylPOSS either.

We tested for similar effects in a system comprised of PEGPOSS dispersed in a melt of PEG of different molecular weights below and above the entanglement molecular weights. Differential scanning calorimetric studies done on the mixtures show linear effects of melting temperature change with respect to PEGPOSS percentages in the mixture. This is illustrated in Fig 3a and Fig 3b. The relative viscosity of the PEGPOSS dispersed in PEG was measured at different molecular weights starting from monomeric (diethylene glycol), 400, 600, 4000 (near entanglement) to 10000 (above entanglement). The lengths of PEG chains on the POSS particle were of a molecular weight of approximately 600. Such a particle would lie at the extreme end of the model that is proposed by Jayaraman and Schweizer where the number of tethers f and the size of the tethers N_p are large and as a resultant are at the high end of the solubility curve. In this case the PEGPOSS is infinitely soluble in PEG of atleast 10000 molecular weight as explored in

this study. Interestingly, the viscosity of the PEGPOSS was almost similar to the viscosity of PEG600 ($2.15*10^{-2}$ Pa.s for PEG 600 versus $2.75*10^{-2}$ Pa.s). The relative viscosities of the mixtures are in line with normal expected mixing rules since at molecular weights lower than 600, the viscosity of the matrix is lower than that of PEGPOSS and a rise in viscosity is seen as PEGPOSS content is increased. At 600, where the viscosity is comparable, the relative viscosity curve is constant near 1. At molecular weights above 600 such as 4000 and 10000, the viscosity seems to drop as would be expected in a simple dilution phenomenon. This is corroborated with the DSC results as mentioned earlier. The entanglement molecular weight of PEG is near around 3000. In fact, when the viscosity versus volume fraction is plotted for PEGPOSS in PEG400 in the low volume fraction limit, and extrapolated to a volume fraction of 1, the resulting viscosity is equal to that of PEGPOSS itself thus showing a linear mixing profile.

Thus in summary, The systems of IsooctylPOSS and IsobutylPOSS dispersed in PDMS and PEGPOSS dispersed in PEG do not conform with the classical colloid rheology models or with Mackay et al's hypothesis of entanglement loss due to confinement.

Wang and Hill[9] attribute the lowered intrinsic viscosity due a zone of lowered viscosity of the polymer matrix from the bulk around the interface of the particle-polymer interaction that extends out to a distance δ with a viscosity η_i and density ρ_i within a bulk matrix medium defined with viscosity η_o and density ρ_o. The degree of slip is defined as k_s and the layer viscosity ratio χ as $(\eta_i/\eta_o)/(\rho_i/\rho_o)$. Keeping $k_s = 1$ for no slip conditions and $\chi = 1$ results in an Einsteinian intrinsic viscosity of $[\eta] = 2.5$. For $\chi = 1$, if $k_s = 0$, $[\eta]$ is found to be 1. For $\chi > 1$ $[\eta]$ is found to exceed 2.5 increasing with respect to δ/D, where D is the diameter of the nano-particle. For $\chi < 1$ however, negative $[\eta]$ values are obtained, which is independent of the fact of whether the polymer chains are entangled or not. This model is thus qualitatively more predictive of the experimental observations made using the POSS-polymer systems in this study since entanglements play no role in the model.

Kim and Zukoski[21] report that $[\eta]$ decreases linearly as a function of ε_{pc} for 44 nm silica particles. This shows that the lowered viscosity around the particle may not be a function of the size of the particle at all. They observe that by extrapolating the trend for an $\varepsilon_{pc} < 0.15$, negative values of $[\eta]$ could be possible. They are not able to accomplish measurements in this region due to limitation imposed by phase separation of the particles at such low values of ε_{pc} due to the large size of the particles. The polymers in this study are below entanglement molecular weight,

reiterating the fact that the mechanism of lowered intrinsic viscosity seems be independent of entanglements.

The intrinsic viscosity of IsooctylPOSS was plotted as a function of Rg of the polymer matrix as shown in Fig 13. below:

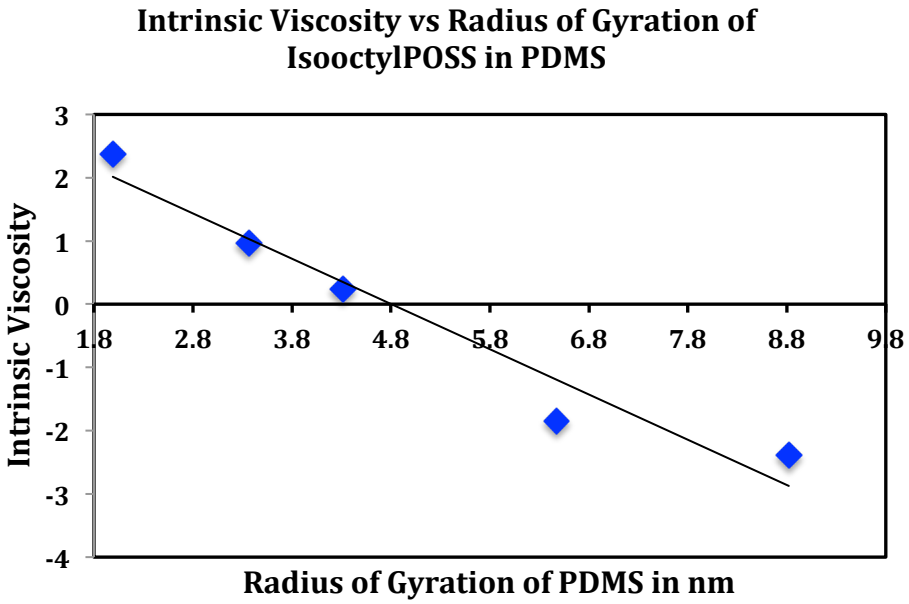

Fig 13. Intrinsic Viscosity of IsooctylPOSS versus Radius of Gyration of PDMS. The linear relation is found to be $[\eta] = -0.715 \pm 0.10 * Rg + 3.43$

Surprisingly, it seen that the intrinsic viscosity varies linearly with Rg. Thus one is led to believe that the distance of the speculated zone of lowered viscosity and density extends out as a linear function of the radius of gyration of the polymer. To test this hypothesis, The Wang and Hill model was plotted to replicate this linearity. Under conditions of $\chi = 0.1$ to approximate a lowered viscosity as seen with the POSS particles, and k=0 for slip perfect slip, and a particle radius of about 1.25 nm to approximate POSS, and varying δ on the size scale of about Rg as seen in PDMS (1-9 nm), $[\eta]$ vs plotted against δ as showin in Fig 14. below:

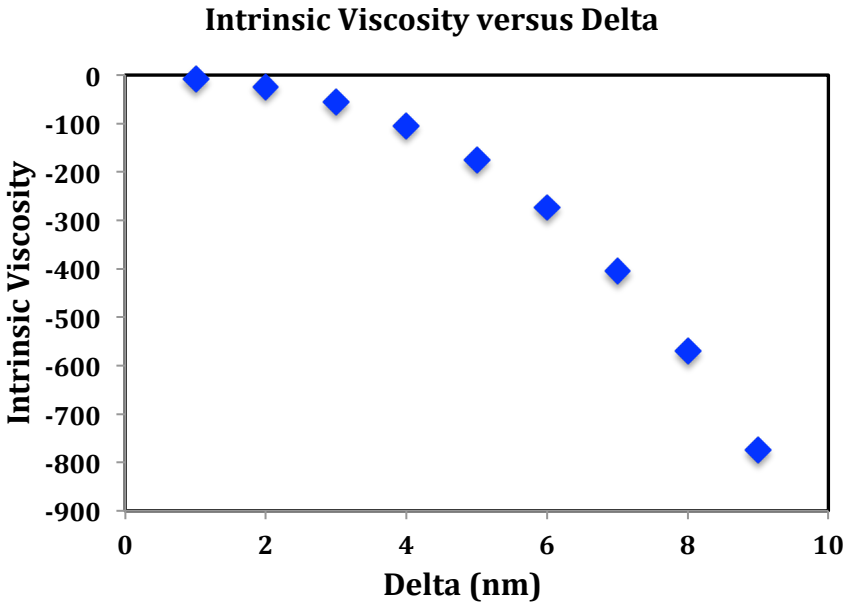

Fig 14. Intrinsic Viscosity [η] versus δ (nm) for δ values comparable to Rg values of PDMS polymer matrix of experimental system

The Intrinsic viscosity in this case is clearly not linear with respect to δ, which in turn is representative of length scales of Rg. Re-plotting the model however for δ values that are an order of magnitude less than Rg values of the experimental system yields the plot show below in Fig 15. that shows an almost linear correlation as seen experimentally for different values of χ = 0.1, 0.5 and 0.7 with lower χ values representing larger drops in viscosity than in bulk. The simulated values of intrinsic viscosities for χ = 0.1 are also similar to what are seen experimentally suggesting a reasonable match between theory and experiment.

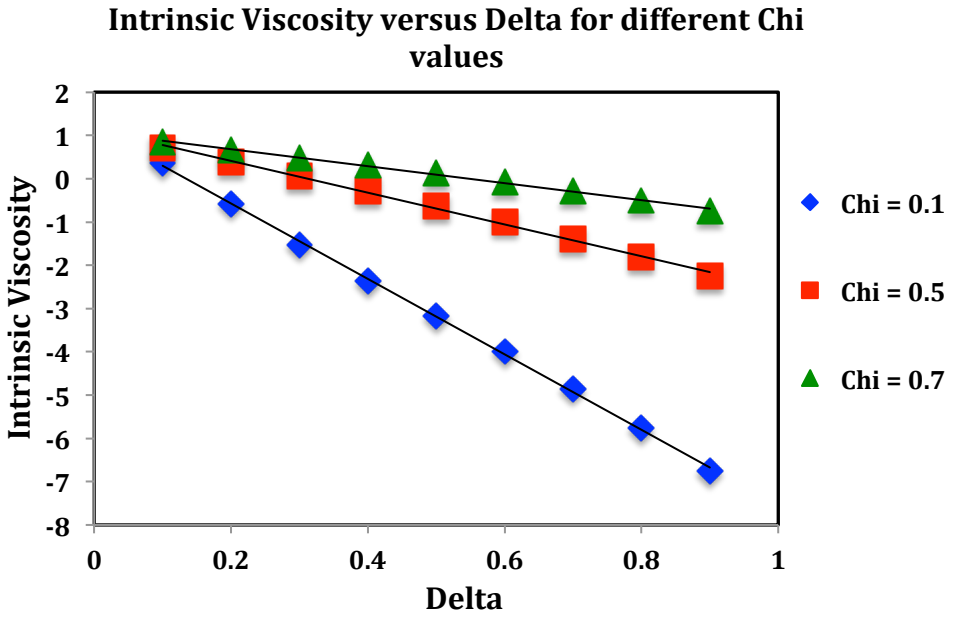

Fig 15. Intrinsic Viscosity [η] vs δ (nm) for δ = 0.1 * Rg values for χ = 0.1, 0.5, 0.7 using the Wang and Hill model. The slope and intercept for the curves are reported in Table 5.

χ	m (slope)	c (intercept)
0.1	-8.71	1.17
0.5	-3.67	1.14
0.7	-1.96	1.07

Table 5. The slopes (m) and intercepts (c) in the linear relation of the form $[\eta] = \delta * m + c$ for different values of χ according to Fig 15.

Thus we can see that the Wang and Hill model describes well, the trend of lowering intrinsic viscosity to negative values as the molecular weight of the polymer matrix chain increases (with δ varying linearly with Rg in the regime where $\delta << Rg$). Also, as the χ value decreases signifying a larger drop in viscosity compared to the bulk, the intrinsic viscosity is seen to become more negative as seen in Fig 15.

Through our understanding of observations by Kim and Zukoski, and simulations based on model proposed by Wang and Hill, we thus hypothesize that lower the ε_{pc} values of particle-polymer segment interactions the greater is the ability of the particle to induce a reduction in intrinsic viscosity down to negative values since a low ε_{pc} would result in a greater reduction in viscosity upto a distance δ resulting in a lower value of χ. Therefore, as ε_{pc} becomes small, χ also becomes small eventually resulting in the intrinsic viscosity being reduced to values less than zero, since at low ε_{pc} values, where there is very little particle-polymer segment interaction, polymer chains are depleted leading to a low viscosity zone around the particle, which is understood as $\chi < 1$ in the Wang and Hill model. The zone of depletion is understood to vary linearly as a fixed fraction of the radius of gyration of the polymer matrix as understood from simulations. Thus we conclude that ε_{pc} as defined in PRISM is related to χ as defined in the model by Wang and Hill.

Although the low ε_{pc} values are necessary to induce the lowering of intrinsic viscosity of the polymer melts, the particles become more insoluble as a result and eventually phase separate as predicted using PRISM theory and confirmed by Anderson and Zukoski[22]. Thus, in order to lower the intrinsic viscosity, a balance must be obtained between the solubility of the particle and the lack of interaction between polymer segment and particle surface. This balance can be enhanced by the use of tethers as is successfully demonstrated in the experiments of the tethered POSS particles in the polymer melts and also predicted by PRISM theory developed for tethered particles by Jayaraman and Schweizer[19]. The tethers introduce a degree of density fluctuations that are able to contribute to entropic mixing to a degree and thus keep otherwise low ε_{pc} systems that should be insoluble, soluble instead.

The length of the tethers is seen to have an influence on the solubility of the particle as well as the ability of the particle to lower intrinsic viscosity. Through the data for IsooctylPOSS and IsobutylPOSS dispersed in 63k molecular weight PDMS, the lowering of the intrinsic viscosity in IsobutylPOSS with smaller tethers is seen to be larger in magnitude compared IsooctylPOSS. Values of $[\eta]$ for Isooctyl tethers are -1.85 whereas it is -7.3 in the case of Isobutyl tethers. This thus experimentally suggests that the ability to lower intrinsic viscosity as the tether length shortens increases for the same value of ε_{pc}. The IsobutylPOSS are considerable less soluble in PDMS (1% by weight) than IsooctylPOSS (20% by weight) independent of

molecular weight of the polymer matrix thus confirming what is predicted in PRISM about longer tethered particles being more soluble independent of molecular weight.

The higher density fluctuations on the surface due to longer tethers essentially renders the surface of the particle "soft" and is thus able to more easily accommodate polymer configurations near the surface making the particle less able to lower the viscosity of polymer near the interface at the same ε_{pc} values. The surface softness is also crucial in keeping the particle stable and preventing depletion aggregation. Thus a balance between ε_{pc} and tether length determines the extent to which the particle is able to lower the intrinsic viscosity of the melt. For extremely long tethers, as in the case of PEGPOSS in PEG of different molecular weights, experiments show a simple mixing effect thus suggesting that at the extreme end of the tether length regime (or very high particle surface softness) the ability of the particle to lower the viscosity is lost.

REFERENCES

1. David Hon and Nobuo Shiraishi, eds. (2001) Wood and cellulose chemistry, 2nd ed. (New York: Marcel Dekker), p. 5 ff

2. "Collagen-Hydroxyapatite Composites For Hard Tissue Repair", DA Wahl, JT Czernuszka, European Cells and Materials, 11, 2006, 43-56

3. P.M. Ajayan, L.S. Schadler, P.V. Braun (2003). Nanocomposite science and technology. Wiley. ISBN 3-527-30359-6

4. "Effect of Ideal, Organic Nanoparticles on the Flow Properties of Linear Polymers: Non-Einstein-like Behavior", Anish Tuteja, Michael E. Mackay, Macromolecules 2005, 38, 8000-8011

5. "A new determination of molecular dimensions", Albert Einstein, Annalen der Physik (ser. 4), 19:289–306, 1906

6. "The determination of the bulk stress in a suspension of spherical particles to order c^2", G.K. Batchelor, J.T. Green, Journal Fluid Mechanics, 56(3), 401–427, 1972

7. "The dependence of suspension viscosity on particle size, shear rate, and solvent viscosity", Pavlik; Marc, DePaul University 2006

8. "A Critical Size Ratio for Viscosity Reduction in Poly(dimethylsiloxane)-Polysilicate Nanocomposites", Randall G. Schmidt, Glenn V. Gordon, C_ecile A. Dreiss, Terence Cosgrove, Val J. Krukonis, Kara Williams, and Paula M. Wetmore, Macromolecules 2010, 43, 10143–10151

9. "Anomalous bulk viscosity of polymer-nanocomposite melts", Mu Wang, Reghan J. Hill, Soft Matter, 2009, 5, 3940–3953

10. "Encyclopedia Britannica", Topic: Brownian Motion, http://www.britannica.com/EBchecked/topic/81815/Brownian-motion

11. "Encyclopedia Brittanica", Topic: Colloids, http://www.britannica.com/EBchecked/topic/125898/colloid

12. Lyklema, J. Fundamentals of Interface and Colloid Science, Vol. 2, p. 3208, 1995

13. IUPAC Compendium of Chemical Terminology, 2nd Edition (1997)

14. "The Huggins Coefficient for the Square-Well Colloidal Fluid", Johan Bergenholtz, Norman J. Wagner, Ind. Eng. Chem. Res., 1994, 33, 2391-2397

15. "PRISM Theory of the Structure, Thermodynamics, and Phase Transitions, of Polymer Liquids and Alloys", K.S. Schweizer, J.G. Curro

16. "Contact Aggregation, Bridging, and Steric Stabilization in Dense Polymer-Particle Mixtures", Justin B. Hooper, Kenneth S. Schweizer, Macromolecules 2005, 38, 8858-8869

17. "Many body effects on the phase separation and structure of dense polymer-particle melts", Lisa M. Hall, Kenneth S. Schweizer, The Journal of Chemical Physics 128, 234901 (2008)

18. "Concentration Fluctuations, Local Order, and the Collective Structure of Polymer Nanocomposites", Lisa M. Hall, Benjamin J. Anderson, Charles F. Zukoski, Kenneth S. Schweizer, Macromolecules 2009, 42, 8435–8442

19. "Effective Interactions, Structure, and Phase Behavior of Lightly Tethered Nanoparticles in Polymer Melts", Arthi Jayaraman, Kenneth S. Schweizer, Macromolecules 2008, 41, 9430-9438

20. "Thermomechanical Properties of Poly(methyl methacrylate)s Containing Tethered and Untethered Polyhedral Oligomeric Silsesquioxanes", Edward T. Kopesky, Timothy S. Haddad, Robert E. Cohen, Gareth H. McKinley, Macromolecules 2004, 37, 8992-9004

21. "Super- and sub-Einstein intrinsic viscosities of spherical nanoparticles in concentrated low molecular weight polymer solutions", So Youn Kim, Charles F. Zukoski, Soft Matter, 2012, 8, 1801–1810

22. "Rheology and Microstructure of an Unentangled Polymer Nanocomposite Melt", Benjamin J. Anderson, Charles F. Zukoski, Macromolecules 2008, 41, 9326-9334

23. "Studying Abnormal Viscosity Behavior in Dilute Oligomer Solutions by SEC and Rheology", André M. Striegel, David B. Alward, Journal of Liquid Chromatography and Related Technologies, Vol. 25, Nos. 13–15, pp. 2003–2022, 2002

24. Hybrid Plastics Catalog, http://www.hybridplastics.com/docs/catalog2011.pdf

25. "Molecular Theory of the Scattering of Light in Fluids". B.H. Zimm, J. Chem. Phys. 13 (4): 141 (1945)

26. "Differential Calorimetry Studies on Poly(ethylene Glycol) with Different Molecular Weights for Thermal Energy Storage Materials", Krzysztof Pielichowski, Kinga Flejtuch, Polymers for Advanced Technologies, 13, 690-696, 2002

27. “Effect of Molecular Weight on Synthesis and Surface Morphology of High-Density Poly(ethylene glycol) Grafted Layers”, Bogdan Zdyrko, Sunil K. Varshney, and Igor Luzinov, Langmuir 2004, 20, 6727-6735

28. Dow Corning Silicones : http://www.dowcorning.com/content/discover/discoverchem/weight-vs-viscosity.aspx

29. “Mean-square radius of gyration of polysiloxanes”, Zhiping Zhou, Deyue Yan, Macromol. Theory Simul., 6, 161-168, (1997)